Galactomannan Gelation: A Thermal and Rheological Investigation Analyzed Using the Cascade Model

P. H. Richardson,* A. H. Clark, A. L. Russell, P. Aymard, and I. T. Norton

Unilever Research Laboratory, Colworth House, Sharnbrook, Bedford MK44 1LQ, U.K.

Received June 30, 1998; Revised Manuscript Received December 22, 1998

ABSTRACT: High-temperature water soluble fractions of locust bean gum with average galactose contents of 15.2% and 16% w/w displayed conventional gelling behavior. Gel properties were dependent on galactose content, gelling temperature and concentration. The gels appeared elastic, failed at up to 150% strain, and exhibited true gellike character with long-lived cross-links. Rheological meltdown occurred over a broad temperature range, and the gels melted at temperatures between 100 and 110 °C. Cascade analysis of the storage modulus vs concentration data gave critical gelling concentrations, $C_o = 0.14-0.24\%$ w/w after 3 months gelation, but this analysis was unable to uniquely determine the number of potential cross-linking forming sites per molecule, i.e., the functionality, f. A value of $f = 5$, as well as average values of the standard molar enthalpy, $\Delta H° = -99.6$ kJ/mol and standard molar entropy, $\Delta S° = -0.201$ kJ/(mol K), for cross-link formation, was subsequently determined through an extension of the cascade formalism to describe modulus vs temperature meltdown data. That these values did not reflect equilibrium melting was shown by a detailed comparison of the analyses of concentration and temperature dependencies of the storage modulus using the cascade model and also by an increase in the number and length of cross-links after 8 months gelation time and by rheological annealing at slower heating rates. An attempt by simulation to assess errors introduced through the assumption of equilibrium gel melting indicated that the true functionality, f, was closer to 20 and that the idealized critical gelling concentrations (were the gels able to reach equilibrium) would be much smaller than the 0.14−0.24% w/w values obtained after 3 months. The simulation also showed that the real values of $\Delta H°$ and $\Delta S°$ were likely to be close to the estimates obtained using the equilibrium theory and nonequilibrium data obtained after 3 months.

I. Introduction

Many gelation studies have been performed on the more conventional biopolymer gelling systems,[1,2] but studies of locust bean gum (LBG) gelation have usually been restricted to systems where LBG is combined with another biopolymer, in the so-called synergistic gelation.[3] On its own, LBG is less well-known for its gelling character. This plant seed galactomannan, whose chemical structure is based on a 1,4-linked β-D-mannan backbone with 1,6-linked α-D-galactose side groups[4] will form gels through freeze/thaw cycling.[5−7] Cross-links are formed through association of galactose uninhibited mannan regions, where the weight average galactose free mannan block length is greater than six monomer units.[8] Gelation also occurs, although at very slow rates, in viscous solutions containing more than 1% solids.[7,9,10] As with all naturally occurring polysaccharides, LBG is polydisperse in terms of its molecular weight and chemistry. Whereas the average galactose content is usually between 20 and 23 wt %, LBG chains may contain both higher and lower levels of galactose. Such chemical polydispersity has been fractionated according to LBG's water temperature solubility, where the gelling capacity of a fraction increases with the temperature required for its dissolution.[7,11,12] The high-temperature soluble fractions contain a lower average galactose content and thus more galactose-free uninhibited mannan regions are available to form mannan/mannan junction zones consistent with the original model proposed by Dea et al.[7] This gelation model was extended by McCleary et al.,[13] who suggested that for mannan/mannan association, the mannan segments need only to be free of galactose side chains on one side of the mannan backbone. More recently, the original model was further developed by Gidley et al.[14] Using CPMAS NMR, in accordance with McCleary et al.,[13] these authors have shown that junction zones in LBG networks are enriched in mannan units and that the mannan does not exist as a 2-fold cellulosic conformation. They concluded that no major conformational change resulted from junction zone formation and that the mannan crystalline structure formed resembled that of Konjac Mannan, i.e., the mannan II polymorph. Furthermore, in addition to the dependence of gelation upon galactose content, the nature of the galactose residue distribution along the mannan backbone also influences galactomannan gelation as reviewed by Morris.[3]

The work described in this paper is part 1 of a systematic study of the gelation of galactomannans using LBG fractionated according to its solubility in water at different temperatures. Here the rheological and thermal properties have been investigated and analyzed in terms of a current biopolymer gelation theory: the cascade model.[15,16]

II. Materials and Methods

Materials. Meyhall locust bean gum was fractionated according to its solubility in water at different temperatures. Using a mechanical stirrer (Ultra-Turrax), 1% w/w LBG was dispersed in deionized water at room temperature. The solution was then heated to 50 °C for 2 h with continuous stirring. After 2 h at 50 °C, the solution was centrifuged at 13000*g* for 30 min. The solute that did not precipitate during centrifugation was deemed soluble. Excess solvent was removed from the decanted supernatant using a rotary evaporator, and the dissolved galactomannan then precipitated in two times the volume of 2-propanol. The precipitate was allowed to stand in

* Address for correspondence: National Starch & Chemical Company, 10 Finderne Av, Bridgewater, New Jersey 08807.

10.1021/ma9810316 CCC: $18.00
Published on Web 02/17/1999

acetone overnight and dried under vacuum at room temperature. The original insoluble fraction was then redispersed in water and heated at 60 °C, with stirring for 2 h. The precipitation procedure described above was repeated. Further fractionation according to the solubility of LBG in water was carried out at 70, 80, 90, and 100 °C. The dried fractions were weighed, and their molecular weight characteristics and average galactose contents, determined. For the molecular weight evaluation, LBG solutions were prepared by first dispersing the polymer in a phosphate buffer (pH = 8) and then heating at 80−90 °C for 30 min with continuous stirring. The phosphate buffer solution was used to dissociate any polymer which had aggregated upon cooling.[17] The molecular weight characteristics were determined using high performance size exclusion chromatography with multiangle laser light scattering (HPSEC−MALLS) ($dn/dc = 0.155$ mL/g), and the average galactose contents were determined using a method by Taylor and Conrad.[18]

Solution and Gel Preparation. Aqueous solutions of the high temperature water soluble fractions of LBG were prepared by initially dispersing the polymer in cold water using a Ultra-Turrax mechanical stirrer. The dispersions were then heated at 90−100 °C for 30 min with continuous stirring using a magnetic stirrer bar. Sodium azide (0.02% w/w) was added to the solutions during solvation to prevent any bacterial growth during gelation. Molecular weight studies found that polymer degradation resulted only if the solutions were mechanically stirred while at 90−100 °C (data not shown). Disklike gel samples for rheological measurements were prepared in inverted 300 mL plastic containers. Solutions were added to the lid portion (6 cm diameter) to a level of approximately 2−3 mm, and then the samples were enclosed using the container portion to prevent moisture loss. In these closed containers, the solutions were held at 12 or 23 °C for 80 and 90 days, for LBG80 and LBG70, respectively. In addition, 1% w/w of LBG70 was left for an extended time, 8 months, at 23 °C.

Small Deformation Rheology. The gelled samples were cut from the lid moulds and carefully transferred onto a rheometer, in this case a Paar Physica UDS200 universal dynamic spectrometer. The computer-controlled gap-setting facility allowed the measurement plates to be moved slowly into position with minimal mechanical damage to the gel. Using 4 cm diameter parallel plate geometry covered with emery paper to prevent slippage, frequency sweeps at 23 °C were performed at 1% strain over 10−0.01 Hz. Either temperature (0.5 Hz and 1 Pa, 1 °C/min) or stress sweeps (0.5 Hz at 23 °C) were then performed. Of the series of high-temperature water soluble fractions, the 60−70 °C (LBG70) and 70−80 °C (LBG80) fractions were studied, as these samples gelled over a practical time scale and appeared to be more readily solvated than higher temperature water soluble fractions. The concentrations studied were from 0.4% to 1.5% w/w, and the samples cured at 12 °C were measured at 23 °C. For the sample held for 8 months at 23 °C, two temperature sweeps were performed (at 1 and 0.1 °C/min).

Differential Scanning Calorimetry. LBG high-temperature water-soluble fractions were cured for 30 days in sample vials at a controlled temperature and then carefully added to the DSC sample pans ensuring maximum contact between gel and sample pan surface. Thermal scans were recorded at 0.5 °C/min from 25 to 120 °C using a Setaram Micro-DSC III differential scanning calorimeter.

Cascade Analysis. The storage modulus vs concentration profiles of gels cured at 12 and 23 °C for both the LBG70 and LBG80 fractions and corresponding melting curves were analyzed using a computer program based on the cascade theory approach to reversible biopolymer gelation[15,16] (see Appendix). The parameters used in this approach include the polymer number average molecular weight (M_n), the number of potential cross-link forming sites per polymer molecule (i.e. the functionality *f*), an equilibrium constant for the junction zone forming process, *K*, and a nonideal front factor "*a*". The front factor allows a free energy contribution aRT energy units ($a > 1$) to the shear modulus rather than RT ($a = 1$) as in the classical (entropic) theory of rubber elasticity. As shown by Clark,[15,16] the nonideal case where the front factor is greater than one, is often shown by biopolymer gels for which the elastically active network chains (EANCs) are stiffer and shorter than the Gaussian chains described by rubber theory.

To apply the cascade model, owing to a strong correlation between *f* and *K*, it was necessary to fix *f* at values such as 3, 100, and 1000 and then to determine corresponding values for "*a*" and *K*. The results of this analysis also yielded values for the critical gelling concentration, C_o (itself a function of *f*, *K*, and M_n). For the gelled samples cured at 12 °C, measurements were performed at 23 °C, and consequently, the temperature input to the cascade model was also 23 °C.

To analyze the rheological meltdown data, an extension to the equilibrium cascade model was used. For both LBG fractions and for the range of concentrations prepared, the storage modulus vs temperature data was analyzed assuming different fixed functionalities. The parameters obtained at any concentration and fixed functionality, *f*, were "*a*" and $\Delta H°$ and $\Delta S°$, the standard molar enthalpy and molar entropy for cross-link formation, respectively, from which the equilibrium constant, *K*, was obtained at each temperature. This value of *K* could then be compared with the *K* obtained from the equilibrium-based modulus-concentration analysis described above. In addition, an estimate of the specific heat capacity, C_p, vs temperature could be determined for comparison with DSC results.

Table 1. Molecular Weight and Average Galactose Contents for Fractionated Components of LBG

LBG fraction	M_n	M_w	M_w/M_n	% galactose	% yield (w/w)
LBG50 <50 °C					65.3
LBG60 50−60 °C	203 000	281 000	1.42	17.6	4.8
LBG70 60−70 °C	246 000	326 000	1.34	16	6.9
LBG80 70−80 °C	201 000	279 000	1.47	15.2	9.4
LBG90 80−90 °C				14.7	3.8
>90 °C				23.6	9.8

III. Results and Discussion

Characterization of Locust Bean Gum. The molecular weight characteristics, the average galactose contents, and the relative amounts obtained for the different temperature water soluble fractions are shown in Table 1. The molecular weight remained relatively constant over the range of high-temperature water soluble fractions measured. As mentioned earlier in the Introduction, the average galactose content decreased as the temperature of water solubility increased. In addition, the majority of LBG was soluble at temperatures below 50 °C, and for the fractions obtained, a maximum in the amount fractionated was found at 70−80 °C (15.2% galactose content). This fractionation and analysis has allowed the galactose polydispersity, i.e., the distribution of galactose content throughout the sample,[22] to be assessed.

Surprisingly, the average galactose content for the fraction obtained at temperatures greater than 90 °C, i.e., 23.6% galactose, was greater than for the other high temperature water soluble fractions. This material may contain LBG chains possessing different distributions of galactose substitution along the mannan backbone resulting in a change in its solubility in water, or more likely, it contains undissociated LBG polymer/polymer associations. As found below, the mannan-mannan associations are highly temperature stable, melting at approximately 100 °C. This undissolved fraction also contained a protein fraction from the leguminous seed.

Cascade Analysis of Modulus vs Concentration Data. Figure 1 displays a series of frequency sweeps

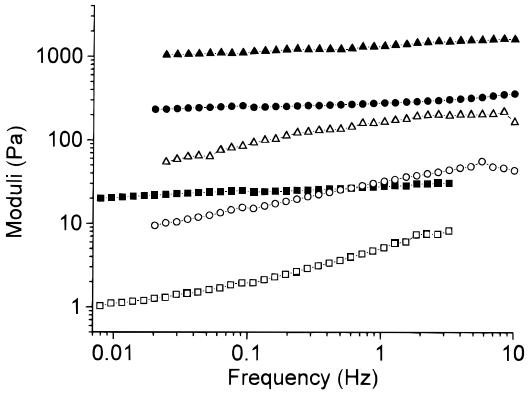

Figure 1. Storage (closed symbol) and loss moduli (open symbol) vs frequency at 0.4% w/w (■), 0.8% w/w (●), and 1.5% w/w (▲) for LBG80 cured at 12 °C for 3 months.

Table 2. Storage Modulus vs Concentration for LBG Fractions LBG70 and LBG80 Cured at 23 and 12 °C, Respectively, for 3 Months

	G' (Pa)			G' (Pa)	
LBG70 concn (% w/w)	23 °C gelation temp	12 °C gelation temp	LBG80 concn (% w/w)	23 °C gelation temp	12 °C gelation temp
0.5	59	51	0.4	28	38
0.6	73	91	0.6	95	98
0.7	108	154			
0.8	172	186	0.8	284	220
1.0	265	221	1.0	720	485
1.2	450	293	1.2	760	
1.5	820	709	1.5	1460	1000

for 1.5%, 0.8%, and 0.4% w/w concentrations of the LBG80 fraction after 80 days at 12 °C. These galactomannan gels displayed relatively frequency independent moduli (over 0.01−10 Hz) typical of gel networks possessing long-lived cross-links, though the loss components were larger than those for other gelling systems,[19−21] i.e., tan $\delta \approx 0.1$. This higher loss modulus could indicate the presence of a sizable sol fraction but it could also arise from network imperfections such as "dangling ends", entanglements, etc., all symptomatic of a low level of cross-linking having been achieved. Table 2 lists the storage moduli for the LBG80 and LBG70 fractions both cured at 12 °C and 23 °C. The higher temperature water-soluble fraction, LBG80, generally produced gels with higher moduli than LBG70 at the equivalent concentration and temperature. This is consistent with the gelation model originally proposed by Dea et al.[7] where the junction zones are formed through galactose-uninhibited mannan/mannan associations. For LBG80, there are either longer and/or more junction zones as this fraction contains fewer galactose residues than LBG70. Additionally, the majority of storage moduli measured were higher for the gels cured at 23 °C than for those cured at 12 °C, which suggests that more cross-links are present for gels prepared at 23 °C. However, this trend is not conclusively established.

Figure 2 displays the modulus-concentration dependence for both fractions cured at 23 °C and the resultant cascade analysis for three fixed functionality, *f*, values, 3, 100, and 1000. The results of these analyses are presented in Table 3. As expected, there is a strong correlation between *f* and *K* results and, as depicted in Figure 2, it was impossible to deduce, over the concentration range studied, which functionality value, *f*, was the optimum. The higher functionality values had lower

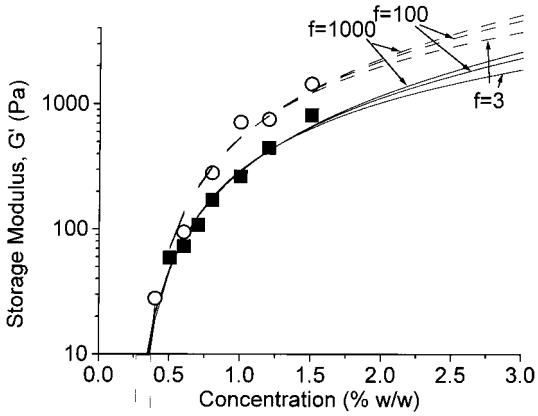

Figure 2. Cascade analysis of the storage modulus vs concentration for LBG80 (○) and LBG70 (■) cured at 23 °C for 3 months. Analysis was performed for three different functionalities, $f = 3$, 100, and 1000.

front factors, which represent more rubber-like junction zones. Possibly, these higher functionalities are more appropriate, as it is expected from earlier chemical structure analyses[13] that the gels possess many short "galactose-free" mannan/mannan associations. The cascade analysis allowed the critical gelling concentrations for gelation to be accurately determined (and independently of assumed *f* values). These ranged from 0.14% to 0.24% w/w depending upon functionality, gelation temperature and galactose content, with the lower galactose containing fraction, LBG80, having an unexpected slightly higher value. This slight discrepancy may be kinetic in origin, as the LBG80 fraction measurements (80 days gelation time) were performed on average 10 days before the LBG70 measurements (90 days gelation time). It suggests that the system has not reached equilibrium and thus the use of an equilibrium based cascade model to describe this gelation process is questionable. This point will be addressed later in more detail.

For the LBG fractions cured at 12 °C, the front factor, "*a*", as well as the critical gelling concentration were lower and *K* was higher than that for gelation at 23 °C. As described in a following paper,[22] the gelation rate for LBG80 and LBG70 was fastest at approximately 10 °C. Consequently, at 23 °C, the LBG fractions will not have gelled to the same extent as at 12 °C. The following paper[22] also shows that after 3 months, both fractions cannot be viewed as fully gelled systems, and this would explain the lower C_o concentrations obtained for fractions gelled faster at the lower gelling temperature, 12 °C. In addition, it might be expected that the type, and number, of junction zones formed at the lower temperature may be different from those formed at 23 °C.

Yield Stress Characteristics. The results of stress sweeps for the LBG80 and LBG70 fractions at different concentrations, and gelation temperatures, are included in Table 4. These gels failed at up to 150% strain with a reduction in yield strain with increasing concentration, a situation where the distance between junction zones decreased.[23] Only one stress sweep was performed for LBG80, and this displayed similar large deformation characteristics as for LBG70.

The gels cured at 12 °C had significantly lower yield strains, approximately 40−50% smaller than at 23 °C, and the storage modulus decayed progressively with applied strain (see Figure 3). This is additional evidence supporting the formation of a different type and/or

Table 3. Results of the Cascade Analysis of the Storage Modulus vs Concentration Relationship for LBG70 and LBG80 Cured at 23 and 12 °C for 3 Months

	LBG70 (16% galactose)		LBG80 (15.2% galactose)	
functionality, f	gelled at 23 °C	gelled at 12 °C	gelled at 23 °C	gelled at 12 °C
$f = 3$	$C_o = 0.214$ $K = 76610$ L/mol $a = 8.56$	$C_o = 0.175$ $K = 93490$ L/mol $a = 6.37$	$C_o = 0.24$ $K = 55750$ L/mol $a = 14.65$	$C_o = 0.193$ $K = 69220$ L/mol $a = 8.71$
$f = 100$	$C_o = 0.193$ $K = 13.1$ L/mol $a = 1.28$	$C_o = 0.149$ $K = 17.0$ L/mol $a = 0.89$	$C_o = 0.229$ $K = 9.03$ L/mol $a = 2.39$	$C_o = 0.178$ $K = 11.65$ L/mol $a = 1.33$
$f = 1000$	$C_o = 0.184$ $K = 0.13$ L/mol $a = 1.12$	$C_o = 0.137$ $K = 0.18$ L/mol $a = 0.73$	$C_o = 0.226$ $K = 0.09$ L/mol $a = 2.20$	$C_o = 0.172$ $K = 0.12$ L/mol $a = 1.17$

Table 4. Rheological Stress and Strain Sweep Results for Gelled LBG80 and LBG70 Fractions[a]

	yield stress and strain	
LBG70 concentration (% w/w)	23 °C gelation temp	12 °C gelation temp
0.6 (LBG80)	73 Pa, 74%	–
0.6	81 Pa, 111%	–
0.7	120 Pa, 111%	–
0.8	190 Pa, 110%	–
1.0	395 Pa, 149%	120 Pa, 54%
1.2	405 Pa, 90%	122 Pa, 42%
1.5	766 Pa, 93%	367 Pa, 52%

[a] Samples were cured for 3 months at 23 and 12 °C (– = no measurement).

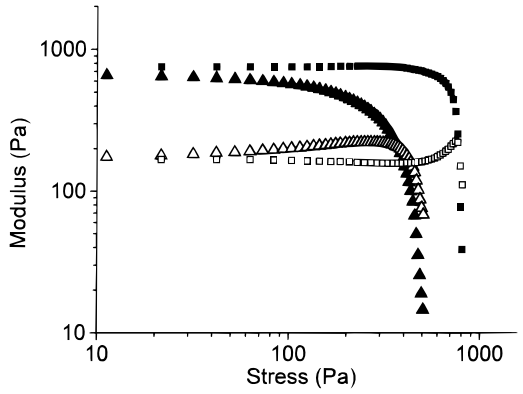

Figure 3. Stress sweeps (at 1 Hz) for 1.5% w/w LBG70 cured at 23 °C ($G' = ■$; $G'' = □$) and 12 °C ($G' = ▲$; $G'' = △$) for 3 months.

number of junction zones at 12 °C with respect to those at 23 °C. The lower yield strain values suggests that the lengths of flexible chains between junction zones are smaller and thus the number of cross-links higher at 12 °C and/or the cross-links formed at 12 °C are more susceptible to higher strains. As the storage modulus was overall larger at 23 °C, the latter explanation seems more likely.

Cascade Analysis of Gel Modulus vs Temperature. Figure 4 displays typical melting profiles for LBG80 and LBG70 at 0.8% w/w, cured at 12 °C. Usually, at temperatures greater than 40−60 °C, the storage modulus decreased gradually as the temperature increased, but somewhat sporadically, several melting profiles displayed an unexpected, abrupt increase in G' prior to the melting period, similar in appearance to the melting profile obtained for concentrated, unfractionated, LBG gels.[10] In the concentrated LBG gel case, the increase in G' was reasoned to be a result of an increase in chain entropy with temperature, whereas an alternative explanation base upon kinetic annealing will be discussed later.

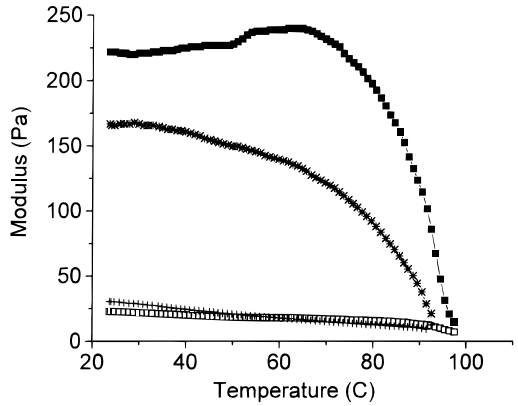

Figure 4. Meltdown curves (at 1 Hz and 1 °C/min) for LBG80 ($G' = ■$; $G'' = □$) and LBG70 ($G' = ∗$; $G'' = +$) cured at 12 °C for 3 months.

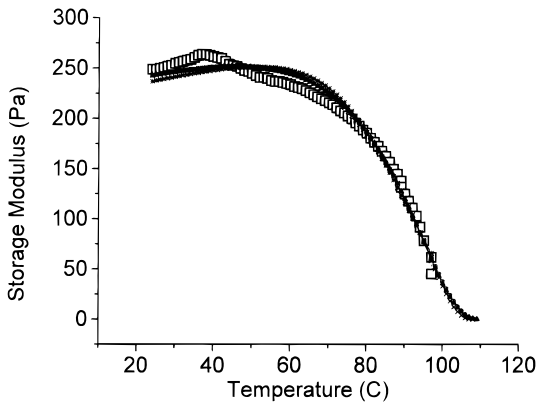

Figure 5. Cascade fit using $f = 3$ (○), $f = 5$ (▲), $f = 10$ (×), and $f = 100$ (∗) for experimental data (□) of storage modulus vs temperature for 0.8% w/w LBG80 cured at 23 °C for 3 months.

The gel melting temperatures (where $\tan \delta = 1$) for these high temperature soluble fractions of LBG were relatively high, i.e., 100−110 °C, which is consistent with the aqueous insolubility seen for mannan, and the high melting temperature, thermoirreversible nature of other mannan-based gels such as deacetylated konjac mannan.[24] The melting transition was broader than that found for gelatin[25] but sharper than that for a low DE (degree of esterification) pectin−calcium gel.[25] LBG80 gels melted at higher temperatures than those from LBG70. The higher melting temperature for systems with lower galactose fraction indicates that these gel networks contain junction zones that are more stable (probably through longer association lengths).

In Figure 5, the cascade fits to the melting data for 0.8% w/w LBG80 cured at 23 °C are displayed for the fixed functionalities, $f = 3$, 5, 10, and 100. The results

Table 5. Results of the Cascade Analysis at Different Functionalities of the Storage Modulus vs Temperature for 0.8% w/w LBG70, Cured at 12 °C for 3 Months

	$f = 3$	$f = 5$	$f = 10$	$f = 20$	$f = 100$
"*a*"	1.32	0.80	0.40	0.193	0.038
ΔH (kJ/mol)	−116.2	−97.1	−123.4	−160.4	−171.1
ΔS (kJ/(mol K))	−0.232	−0.197	−0.284	−0.393	−0.437
T_m (°C)	103.7	104.2	102.4	102.8	115.4
Σ	0.033	0.031	0.024	0.053	0.153
heat output (J/g)	1.42	1.97	5.02	13.05	69.5

of these analyses and others for different LBG concentrations and gelling temperatures are summarized in Tables 5 and 6. The average enthalpy of cross-link formation was −99.6 kJ/mol of cross-links, which is intermediate between values obtained for gelling biopolymers such as a low DE pectin[26] (−7.5 ± 0.8 kJ/mol) and gelatin[25] (−836 kJ/mol). The average entropy of cross-linking, $\Delta S = -0.201$ kJ/(mol K), was also intermediate in value between the low DE pectin[26] (+0.08 to −0.08 kJ/(mol K)) and gelatin[25] (−2.5 to −3.3 kJ/(mol K)). This relatively small entropic change concurs with previous NMR work,[14] which established that no major conformational change occurred during gel formation. Furthermore, as galactomannan chains are quite persistent and rigid in solution,[27] the entropy penalty upon cross-link formation would be small.

All functionalities, *f*, gave curves which fitted closely to the experimental data (see Figure 5) and in contrast to the gel modulus vs concentration analyses, here it was possible to distinguish between different functionalities. Least-squares analysis showed that $3 < f < 8$ gave the best fits, with $f = 5$ often being the optimum; see Σ, (defined as the sum-of-squared differences between observed and calculated log G' values, divided by the number of observations), in Table 5. In view of the close to random distribution of galactose residues along the mannan backbone,[13] this result seems unexpectedly low. As will be demonstrated later, this low *f* value is a consequence of the nonequilibrium nature of the gels formed, even after 3 months gelation, and the inappropriate application of an equilibrium model.

Further work involving comparison of the meltdown analyses with the modulus vs concentration results led to some valuable insights into the nature of these LBG gels. In the meltdown treatment, the value of "*a*" obtained for any *f* value was much lower than the corresponding "*a*" value determined from the modulus vs concentration cascade analysis. Analogous to the front factor discrepancy, the equilibrium constant, *K*, from the melting analysis, was much greater than from that based on the modulus vs concentration data suggesting that the critical gelling concentration, C_o, ought to be much smaller than 0.14−0.24% w/w discussed earlier. Once again, these discrepancies could be due to the kinetic nature of the LBG gels as explained in a later section.

The kinetic nature of the gels was further probed by measuring rheological melting profiles at 1 °C/min on 1% w/w LBG70 cured at 23 °C for the longer period of 8 months, and at the slower heating rate of 0.1 °C/min (see Figure 6). When the 1 °C/min scan rate data were analyzed, it was found that the cascade fits were similar to those in Figure 5, and again the optimum functionality was $f = 5$. However, the additional 5 months gelation time at 23 °C for 1% w/w LBG70 clearly showed that continual slow gelation was occurring for these polysaccharides as there was an increase in storage modulus from 265 to 520 Pa (at 1 Hz) and also increases in derived values for $\Delta H°$ and the gel melting temperature (see Table 6). Such increases in G' and $\Delta H°$ suggest that the cross-links increase both in number and in length. Significantly, the slower melting run displayed a steeper increase in G' at temperatures prior to gel melting, indicating that the gels were able to anneal at this slower heating rate. Such kinetically controlled melting provides a possible explanation for the observed sporadic increases in G' prior to melting sometimes observed and discussed earlier.

Differential Scanning Calorimetry. Figure 7 displays differential scanning calorimetry profiles at 0.5 °C/min for LBG80 cured at 10 °C for 30 days, and the results of all DSC experiments are listed in Table 7. As with the rheological measurements, the peak melting temperatures were high, but no clear melting temperature/concentration dependency was found such as predicted by Eldridge and Ferry.[28] The lower galactose LBG fraction, LBG80, melted at approximately 94 °C, slightly higher than LBG70, in accordance with the current LBG gelation model.[7] The DSC melting transition appeared to cover a narrower range than the rheological melting (i.e. a 6−8 °C temperature range) with a lower enthalpy of approximately 1 J/g of polymer after 30 days gelation (see Table 7). As with the rheological data, after 8 months, the extent of gelation had significantly increased, as displayed by a 5.2 J/g melting enthalpy. However, after only 3 days gelation, the melting enthalpy was comparable to that after 30 days. A possible explanation is that some chain segments are able to associate relatively quickly but do not contribute significantly to network formation (i.e. to the gel modulus). Earlier work studying the intrinsic viscosity of LBG also suggested a relatively rapid aggregation process once a hot solution of LBG was cooled from 95 °C.[17,29]

Comparison of DSC and Rheological Melting. Cascade analysis of the rheological meltdown for the LBG fractions enabled an appropriate evaluation of the specific heat capacity, C_p, and thus the heat output as a function of temperature. Figure 8 displays the influence of different choices of functionality, i.e., $f = 3$, 5, and 10 upon the calculated heat output vs temperature based on analysis of data for 1% LBG70 cured at 23 °C for 8 months and then melted at 1 °C/min. The calculated peak melting temperature shifted to lower temperatures as *f* increased, since only a small proportion of cross-links are necessary to form an incipient network at high functionality. Also, as expected, the total melting enthalpy increased as the assumed functionality increased. A comparison of the theoretical heat output profile obtained from analysis of the rheological melting with the experimental heat output from DSC provided, due to the dependence of the peak melting temperature on functionality, a method to determine the functionality of a gelled system, assuming that the heat output from DSC was directly related to cross-link melting. As shown in Figure 8, whereas the experimental DSC peak was much sharper, with a larger melting enthalpy (see Tables 6 and 7), the peak temperatures coincided at $f = 5$. This was the same functionality value obtained earlier from fit quality assessment of the cascade analysis of the rheological meltdown data. The difference in peak sharpness and melting enthalpy, however, may be a result of incorrectly assuming that the DSC melting endotherm is directly linked to the rheological

Table 6. Results of the Cascade Analysis at $f = 5$ of the Storage Modulus vs Temperature for Gelled LBG Fractions Cured for 3 and 8 Months (in *Italics*)

	LBG80 0.6% 12 °C	LBG80 1.5% 12 °C	LBG80 0.8% 23 °C	LBG80 1.2% 23 °C	LBG70 0.6% 12 °C	LBG80 0.8% 12 °C	LBG70 1.0% 23 °C	*LBG70 1.0% 23 °C*
"*a*"	0.51	1.61	0.99	1.96	0.49	0.88	1.48	*0.62*
ΔH (kJ/mol)	−56.9	−125.6	−108.4	−101.3	−107.6	−203	−100.9	*−123.3*
ΔS (kJ/(mol K))	−0.080	−0.276	−0.226	−0.209	−0.226	−0.486	−0.209	*−0.241*
T_m (°C)	135.7	109.5	110.2	112.3	100.9	101.1	105.7	*110.6*
Σ	0.01	0.11	0.037	0.048	0.20	0.019	0.006	*0.033*
heat output (J/g)	1.42	3.14	2.72	2.51	2.18	5.06	2.05	*2.47*

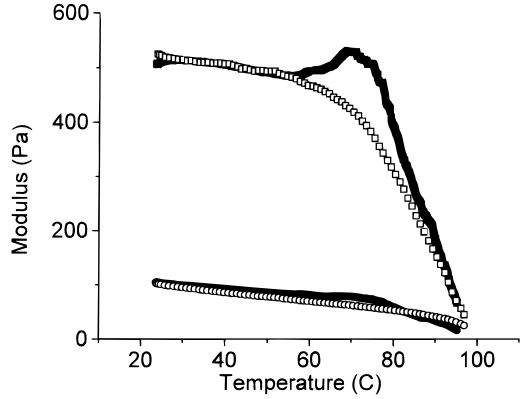

Figure 6. Moduli vs temperature at 1 °C/min (□) and 0.1 °C/min (■) for 1% w/w LBG70 cured at 23 °C for 8 months. Storage modulus, G', was always greater than the loss modulus, G''.

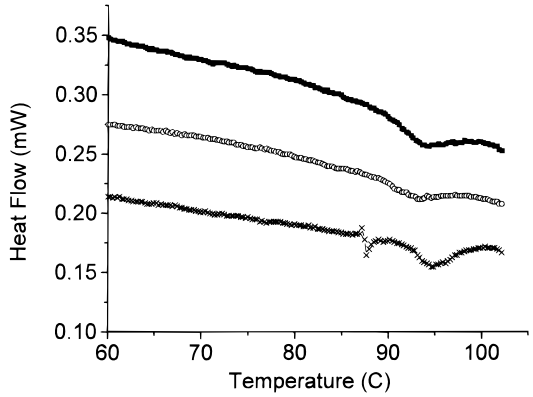

Figure 7. DSC heat flow curves (at 0.5 °C/min scan rate) for 0.5% w/w (×), 0.7% w/w (○), and 2.0% w/w (■) LBG80 cured at 10 °C for 30 days.

melting. As suggested by the large melting endotherm after only 3 days gelation time, the system is highly polydisperse with a small fraction of low galactose containing chains associating early and not contributing to the gel modulus. This additional enthalpic contribution for the LBG gel fractions would seem to invalidate the use of this method of comparing DSC and rheological meltdown to determine f. In consequence, it seems the same f values found by these two different methods may be purely coincidental. Although this comparison method for obtaining the normally elusive functionality of a gelling polymer may not be applicable here, it may be applied more successfully to other gelling systems.

IV. Gelation Model

Contradictions in "*a*", and K and thus C_o, between results obtained from modulus vs concentration and those obtained from modulus vs temperature have already been mentioned. As discussed above, the observed annealing effect upon slower heating and the increase in G' and $\Delta H°$ after 8 months gelation, as well as the large hysteresis between setting and melting temperatures for these LBG fractions, already suggest strong kinetic control. Thus, the direct use of the equilibrium-based cascade model seems inappropriate. However, the fits of storage modulus vs concentration displayed in Figure 2 could still be explained in terms of a kinetic model involving a competition between cross-linking and cyclization (no reversal of either process), resulting in the same predicted curve shape. The constant, K, would then be a kinetic parameter equal to the ratio of the rate constants for the two processes, and C_o and "*a*" would still have their usual meaning. In the case of the modulus−meltdown analysis, the (equivalent) model required to treat the kinetically determined gel case is now more complex as additional equilibrium contributions are present at higher temperatures as the gel melts. To model such a complex kinetic process, introduction of cross-linking reversibility at higher temperatures and effects dependent upon rate of temperature scanning would be required. This is not easily done, and no such model is currently available, but some idea of how the equilibrium model would be expected to fail when applied to gels formed under kinetic control was indicated by the following computer simulation experiment: an "ideal" LBG molecule was imagined with $M_n = 246\,000$ and $\Delta H° = -168$ kJ/mol cross-links, $\Delta S° = -0.418$ kJ/(mol K) cross-links, and $a = 3$, $f = 20$. Ideal melting curves of gel modulus vs temperature were constructed for $C = 0.5$, 1.0, 1.5, and 2.0% w/w using equilibrium theory. It was then assumed that at concentrations $C = 0.5\%$ the system could only achieve a fraction of the equilibrium modulus (G_e) result at 23 °C due to steric hindrance, i.e., kinetic control. It was then assumed that during melting this G_e value remained constant until the ideal equilibrium melting curve value of G_e was met at some upper temperature. The system then followed equilibrium melting after that (see Figure 9). Similar idealized kinetic melting curves were constructed at the other concentrations based upon a concentration dependence of the modulus assuming $a = 3$, $f = 20$ and a chosen value of K (treated as a kinetic parameter). K was chosen so that the modulus starting values at each concentration were much smaller than the ideal equilibrium starting values and more or less consistent with the LBG experimental data. All four sets of kinetic data for modulus vs temperature profiles were analyzed using the (incorrect) equilibrium model, i.e., to simulate what had actually been done when analyzing the real LBG meltdown data. The results showed the following.

(1) The $f = 5$ description gave significantly better fits to the simulated data in all cases than the true $f = 20$ value actually assumed when setting up the equilibrium melting curves. The higher value of 20 is actually more

Table 7. Differential Scanning Results at 0.5 °C/min for LBG70 and LBG80 Cured at 10 °C for 30 Days[a]

LBG70 concn (% w/w)	initial T_m (°C)	peak T_m (°C)	ΔH (J/g of LBG70)	LBG80 concn (% w/w)	initial T_m (°C)	peak T_m (°C)	ΔH (J/g of LBG80)
0.4				0.5	92.4	94.8	1.2
0.6		94.0		0.7	89.4	93.1	1.14
0.8	83.8 [85.2]	92.6 [88.2]	1.33 [1.22]	1.0	88.9	94.0	1.65
1.0	82.2 [[92.5]]	93.0 [[94.7]]	1.08 [[5.2]]	1.5			
1.5	91.0	93.2	0.90	2.0	89.5	93.6	0.85

[a] Key: brackets, cured at 2 °C for 3 days; double brackets, cured at 23 °C for 8 months.

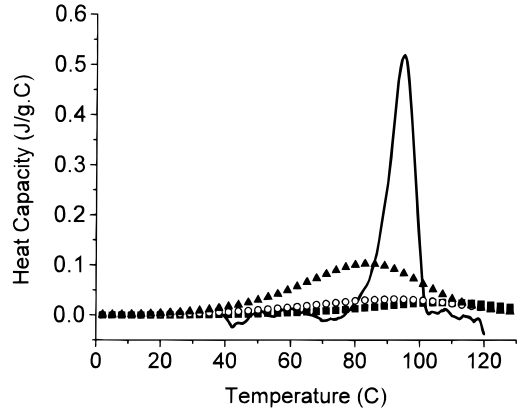

Figure 8. Heat capacity comparison of DSC (—, 0.5 °C/min scan rate) and rheological (1 °C/min scan rate) meltdown of 1% w/w LBG70 cured at 23 °C for 8 months. Key: (■) $f = 3$; (○) $f = 5$; (▲) $f = 10$.

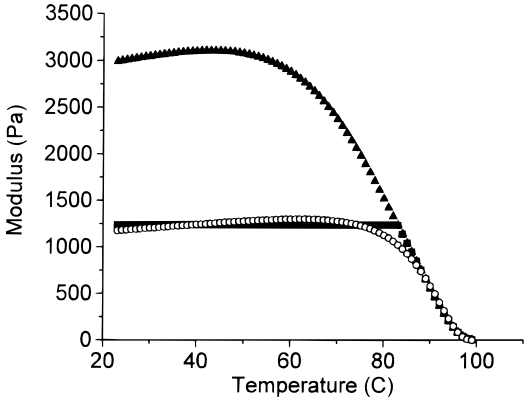

Figure 9. Computer simulation of melting an idealized LBG gel, $M_n = 246\,000$, $\Delta H° = -168$ kJ/mol, $\Delta S° = -0.418$ kJ/(mol K), and $C = 0.5\%$. (▲ = G' at equilibrium melting curve, ■ = G' under kinetic control, constant G' values until the equilibrium melting curve was reached, ○ = G' calculated from cascade anaylsis (equilibrium model) of the kinetic data).

consistent with previous chemical structural analyses inferring that there are many possible cross-link forming sites along a LBG backbone.[11]

(2) "*a*" varied with concentration, and increased with increasing concentration for a given f fit. Also, this calculated front factor was generally smaller than that assumed when constructing the simulated data.

(3) $\Delta H°$ and $\Delta S°$ varied with assumed functionality, and $\Delta H°$ was about 1.5 times greater in absolute value than the value used to calculate the simulated data. These parameters did not vary much with concentration however.

(4) The apparent K value from $\Delta G° = \Delta H° - T\Delta S°$ was much greater (C_o much smaller) than found from equilibrium cascade fitting to the 23 °C modulus vs concentration data assumed when constructing the simulated data.

(5) DSC peaks were sharper for the simulated data than expected for true equilibrium melting using the input parameters but were still a lot broader than the LBG experimental data, so this discrepancy was not fully explained by the simulation.

It can be concluded that while fitting the meltdown data by an equilibrium model approach at first sight seems to be satisfactory, close inspection of the results in relation to a modulus-concentration fit of the starting low temperature values, together with certain parameter variations with concentration, and a disagreement with experimental DSC data, all point to an inadequacy of the cascade equilibrium approach in the context of kinetically determined gels. Doubt is cast on the exact values of parameters such as "*a*", $\Delta H°$, $\Delta S°$, and f extracted from meltdown data by an equilibrium approach, though simulation shows that they may not be vastly different from "true" values for the polymer involved (in this case, LBG fractions, LBG80 and LBG70). To improve this situation a much more complex kinetic model would need to be developed which described the effects of temperature scanning on a LBG cross-linked system initially gelled under kinetic control. It is not clear, however, whether even this model could explain the very sharp DSC melting peak since this sharpness seems inconsistent with the shape of the experimental modulus vs temperature curves themselves. As discussed above, a likely explanation is that these LBG fractions contain a proportion of high melting ordered material, which does not contribute significantly to the rheological melting.

V. Conclusions

The gelation of galactomannans fractionated from locust bean gum with average galactose contents of 15.2% and 16% w/w was dependent on concentration, temperature, and average galactose content. These dependencies are consistent with earlier models based upon association of unsubstituted mannan regions. The large temperature hysteresis between gelation temperature and gel melting and the observed annealing effects at slower scan rates indicate that the gelation mechanism is closely related to polymer crystallization and is under kinetic control. The increase in G' and $\Delta H°$ for cross-link formation indicated that the length in addition to the number of cross-links increased with time. Furthermore, the apparent larger number of cross-links formed at 12 °C, as opposed to 23 °C, supports this crystallization mechanism, as nucleation is favored at the lower temperature. Further developments to this crystallization model are presented in a later paper,[22] which studies the kinetics of gelation of the LBG fractions.

The gels from high-temperature water soluble LBG fractions yielded at up to 150% strain and exhibited true gel like character with long-lived cross-links. Gelation was very slow, progressing over several months, and the

gels melted at temperatures close to 100 °C. Rheologically, the melting transition was broad, covering up to 40 °C, whereas the DSC melting occurred over less than 10 °C. This discrepancy, along with a relatively large DSC enthalpy after short gelation times, suggested that part of the enthalpic associations present in the sample were not involved in cross-link formation, and the DSC enthalpy (associated with cross-linking) at lower temperatures was probably obscured by baseline uncertainty. Such structural polydispersity was also evaluated by measuring the amount of LBG that was soluble at different solvation temperatures in water. Critical gelling concentrations were found to be approximately 0.2% w/w, as assessed after 3 months of gelation. However the gels formed were still under kinetic control, and thus their true C_o values were likely to be much smaller. Near equilibrium was only achieved at higher temperatures during meltdown, and the meltdown analysis determined a large standard enthalpy of cross-link association ($\Delta H° = -99.6$ kJ/mol) with only a small change in corresponding entropy ($\Delta S° = -0.201$ kJ/(mol K)). Whereas these thermodynamic values were obtained by applying an equilibrium theory on meltdown data of a gel which had not attained equilibrium, a computer simulation generating data possessing both kinetic and equilibrium features as the gel melted showed that they were not far from their true values.

A method to determine the functionality of a gelling polymer through comparison of DSC data and rheological meltdown data was also described but found inappropriate for the LBG system studied here.

Acknowledgment. The authors would like to thank their colleagues from Colworth House for many helpful comments and advice and Unilever Research for permission to publish this work.

Appendix

The cascade treatment of biopolymer gelation[15,16,25,30,31] concludes that the shear modulus G is given by

$$G = \{Nf\alpha(1 - v)^2(1 - \beta)/2\}aRT \qquad (1)$$

where $N = C/M$, C being the concentration in mass terms and M the molecular weight. F is the number of sites (or functionalities) per molecule potentially available for cross-linking, and α is the fraction of such sites which have reacted at any time. v and β are given by

$$v = (1 + \alpha + \alpha v)^{f-1} \qquad (2)$$

and

$$\beta = (f - 1)\alpha v(1 - \alpha + \alpha v) \qquad (3)$$

where v is the so-called "extinction probability".[15] The expression in parentheses in (1) then measures the number of moles of elastically active chains per unit volume, i.e., load-bearing elements of the network.[15] In (1), aRT is the average contribution per mole of such chains to the free energy increase in unit strain. For ideal rubbers $a = 1$, but it can be much higher for biopolymers and can depend on temperature, T.

For a gel setting up to a final state, α is calculated in terms of f, C, M, rate constants for the cross-linking process, and time.[31] If cross-linking is reversible, the relevant rate constants are for pairwise cross-linking and its reverse. If, however, irreversible cross-linking occurs, the constants refer to the forward step, as before, and to a process of cross-link wastage (cyclization, steric hindrance, etc.). A second-order forward step is usually assumed, with reversal, or wastage, being first order. The final long-time modulus value G ($t = \infty$) is therefore expressed via EbN (1) in terms of C, M, f, "a", and α ($t = \infty$), which is itself a function of these variables, and also of the ratio of rate constants, K. The modulus G vs C ($t = \infty$) relationship can thus be modeled in terms of f, "a", and K, with M usually assumed known. The concept of a critical concentration, C_o, below which $G = 0$, then readily arises from the condition at the gel point that $\alpha = 1/(f - 1)$, a value which cannot be achieved below C_o, by the kinetics assumed.[16,25,30,31] A nonlinear least-squares computer program was written to perform such data fitting in terms of variables f, K, and "a". In practice, f was normally poorly determined, and fitting was restricted to K and "a", with f constant. There was thus an inevitable indeterminacy in K and "a", unless f could be assigned in an independent manner.

For the situation of gel melting also studied here, it was assumed that the observed fall in modulus with temperature, at fixed concentration C, implied that K could be interpreted as an equilibrium constant (but see discussion in main paper). The temperature dependence of K would then be expected to be[25]

$$K = \exp(\Delta S°/R)\exp(-\Delta H°/RT) \qquad (4)$$

i.e. in terms of a standard enthalpy and entropy of cross-linking. Using eq 1, and assuming constant C and M, it was possible to least-squares fit G vs T data in terms of $\Delta H°$, $\Delta S°$, and "a" (f being fixed for a particular f-model). The predicted critical "melting point" of the gel was also output, together with an estimate for the DSC melting profile based on the calculated cross-link enthalpy and the change in α with temperature. The computer programs could be used both to analyze experimental data and to construct G vs C and G vs T theoretical curves, based on trial values of parameters, a feature used in the simulation described earlier.

References and Notes

(1) Whistler, R. L.; BeMiller, J. N. *Industrial Gums*, 3rd ed.; Academic Press: San Diego, CA, 1993.
(2) Harris, P. *Food Gels*; Elsevier Applied Sci.: New York, 1990.
(3) Morris, E. R. In *Food Gels*; Harris, P., Ed.; Elsevier Applied Sci.: New York, 1990; Chapter 8, pp 291−360.
(4) Dea, I. C. M.; Morrison, A. *Adv. Carbohyd. Chem. Biochem.* **1975**, *31*, 241.
(5) Maier, H.; Anderson, M.; Karl, C.; Magnuson, K.; Whistler, R. L. In *Industrial Gums*; Whistler, R. L., BeMiller, J. N., Eds.; Academic Press: San Diego, CA, 1993; Chapter 8, pp 181−226.
(6) Bayerlein, F. *Plant Polym. Carbohydr.* **1993**, 191.
(7) Dea, I. C. M.; Morris, E. R.; Rees, D. A.; Welsh, J.; Barnes, H. A.; Price, J. *Carbohydr. Res.* **1977**, *57*, 249−272.
(8) Dea, I. C. M.; Clark, A. H.; McCleary, B. V. *Food Hydrocolloids* **1986**, *1*, 129.
(9) Garnier, C.; Schorsch, C.; Doublier, J. L. *Carbohydr. Polym.* **1995**, *28*, 313−317.
(10) Richardson, P. H.; Norton, I. T. *Macromolecules* **1998**, *31*, 1575−1583.
(11) Dea, I. C. M.; Clark, A. H.; McCleary, B. V. *Carbohydr. Res.* **1986**, *147*, 275−294.
(12) Mannion, R. O.; Melia, C. D.; Launay, B.; Cuvelier, G.; Hill, S. E.; Harding, S. E.; Mitchell, J. R. *Carbohydr. Polym.* **1992**, *19*, 91−97.
(13) McCleary, B. V.; Clark, A. H.; Dea, I. C. M.; Rees, D. A. *Carbohydr. Res.* **1985**, *139*, 237−260.
(14) Gidley, M. J.; McArthur, A. J.; Underwood, D. R. *Food Hydrocolloids* **1991**, *5*, 129−140.

(15) Gordon, M.; Ross-Murphy, S. B. *Pure Appl. Chem*. **1975**, *43*, 1−26.
(16) Clark, A. H. In *Food Structure and Behaviour*; Lillford, P. J., Blanshard, J. M. V., Eds.; Academic Press: London, 1987; pp 13−34.
(17) Richardson, P. H.; Wilmer, J.; Foster, T. J. *Food Hydrocolloids* **1998**, *12*, 339−348.
(18) Taylor, R. L.; Conrad, H. E. *Biochemistry* **1972**, *11*, 1383−1388.
(19) Piculell, L.; Nilsson, S.; Muhrbeck, P *Carbohydr. Polym*. **1992**, *18*, 199−208.
(20) Clark, A. H.; Richardson, R. K.; Robinson, G.; Ross-Murphy, S. B.; Weaver, A. C. *Prog. Food Nutr. Sci.* **1982**, *6*, 149−160.
(21) Chronakis, I. S.; Picullel, L.; Borgström, J. *Carbohydr. Polym*. **1996**, *31*, 215−225.
(22) Richardson, P. H.; Aymard, P.; Clark, A. H.; Foster, T. J.; Norton, I. T. To be submitted to *Macromolecules*.
(23) Ross-Murphy, S. B. In *Biophysical Methods in Food Research Critical Reports on Applied Chemistry 5*; Chan, H. W. S., Ed.; SCI/Blackwell Scientific: Oxford, England, 1984; pp 138−199.
(24) Case, S. E.; Knopp, J. A.; Hamann, D. D.; Scxhwartz, S. J. In *Gums and Stabilisers for the Food Industry 6*; Phillips, G. O., Williams, P. A., Wedlock, D. J., Eds.; Oxford University Press: Oxford, England, 1992; pp 489−500.
(25) Clark, A. H.; Evans, K. T.; Farrer, D. B. *Int. J. Biol. Macromolecules* **1994**, *16*, 125−130.
(26) Clark, A. H.; Farrer, D. B. *Food Hydrocolloids* **1996**, *10*, 31−39.
(27) Robinson, G.; Ross-Murphy, S. B.; Morris, E. R. *Carbohydr. Res.* **1982**, *107*, 17−32.
(28) Eldridge, J. E.; Ferry, J. D. *J. Phys. Chem*. **1954**, *58*, 992−995.
(29) Goycoolea, F. M.; Morris, E. R.; Gidley, M. J. *Carbohydr. Polym*. **1995**, *27*, 69−71.
(30) Clark, A. H.; Ross-Murphy, S. B. *Br. Polym. J*. **1985**, *17*, 164−8.
(31) Clark, A. H. *Polym. Gels Networks* **1993**, *1*, 139−58.

MA9810316